This article was downloaded by:
On: *28 January 2011*
Access details: *Access Details: Free Access*
Publisher *Taylor & Francis*
Informa Ltd Registered in England and Wales Registered Number: 1072954 Registered office: Mortimer House, 37-41 Mortimer Street, London W1T 3JH, UK

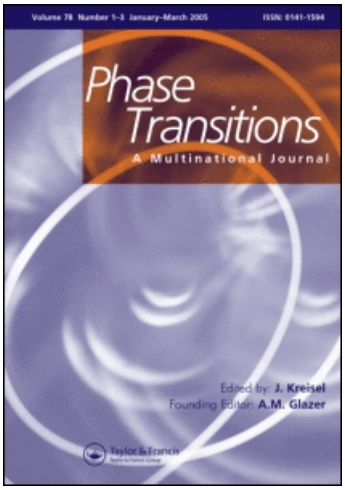

Phase Transitions
Publication details, including instructions for authors and subscription information:
http://www.informaworld.com/smpp/title~content=t713647403

Experimental Study of Disorder-influenced First-Order Transitions in Vortex Matter and in Magnetic Systems

S. B. Roy[a]; P. Chaddah[a]
[a] Low Temperature Physics Laboratory, Centre for Advanced Technology, Indore - 452 013, India

To cite this Article Roy, S. B. and Chaddah, P.(2004) 'Experimental Study of Disorder-influenced First-Order Transitions in Vortex Matter and in Magnetic Systems', Phase Transitions, 77: 8, 767 — 790
To link to this Article: DOI: 10.1080/01411590410001690891
URL: http://dx.doi.org/10.1080/01411590410001690891

PLEASE SCROLL DOWN FOR ARTICLE

Full terms and conditions of use: http://www.informaworld.com/terms-and-conditions-of-access.pdf

This article may be used for research, teaching and private study purposes. Any substantial or systematic reproduction, re-distribution, re-selling, loan or sub-licensing, systematic supply or distribution in any form to anyone is expressly forbidden.

The publisher does not give any warranty express or implied or make any representation that the contents will be complete or accurate or up to date. The accuracy of any instructions, formulae and drug doses should be independently verified with primary sources. The publisher shall not be liable for any loss, actions, claims, proceedings, demand or costs or damages whatsoever or howsoever caused arising directly or indirectly in connection with or arising out of the use of this material.

Phase Transitions
Vol. 77, Nos. 8–10, August–October 2004, pp. 767–790

Taylor & Francis
Taylor & Francis Group

EXPERIMENTAL STUDY OF DISORDER-INFLUENCED FIRST-ORDER TRANSITIONS IN VORTEX MATTER AND IN MAGNETIC SYSTEMS

S.B. ROY and P. CHADDAH*

Low Temperature Physics Laboratory, Centre for Advanced Technology, Indore – 452013, India

(Received 5 February 2004)

Downloaded At: 12:30 28 January 2011

First-order transitions are frequently characterised by hysteresis as the control variable (which may be temperature T, or pressure P, or magnetic field H) is varied across the transition value T_C (or P_C, or H_C). This arises due to supercooling/superheating, with the existence of metastable states giving rise to hysteresis in physical properties. We shall present some of our recent studies on metastable states formed across a first-order transition in vortex matter, and also across a first-order magnetic transition. We shall discuss how quenched-in static disorder influences the nature of this transition process, and highlight the generality of such phenomena in other areas of condensed matter physics.

Keywords: First-order transition; Hysteresis; Quenched disorder; Vortex matter

1. INTRODUCTION

According to the Ehrenfest classification of phase transitions, a first-order phase transition (FOPT) is accompanied by a discontinuity in the first derivative of the free energy, taken with regard to the control variables that can cause the phase transition. In case the control variables are temperature (T) and magnetic field (H), one can report a FOPT across a $T_C(H)$ line if one observes a discontinuous change in entropy (i.e. measures a latent heat) or observes a discontinuous change in magnetisation (M), as one crosses this $T_C(H)$ line by varying either of the control variables T or H. The FOPT would be firmly established if the magnetisation jump and the latent heat satisfy the Clausius–Clapeyron relation. These stringent requirements pose experimental difficulties when the latent heat is small, and it becomes difficult even to distinguish it from a peak in specific heat (White and Geballe, 1979). In such cases the characteristic feature of hysteresis, in a physical property, which varies sharply between the two phases, is used to identify a FOPT (White and Geballe, 1979). This hysteresis seen as T (or H) is decreased and increased around the $T_C(H)$ line is believed to be associated with supercooling or superheating, which can be seen across FOPT (only) when energy

*Corresponding author. E-mail: chaddah@cat.ernet.in

ISSN 0141-1594 print: ISSN 1029-0338 online © 2004 Taylor & Francis Ltd
DOI: 10.1080/01411590410001690891

fluctuations are small. The identification of such metastable (supercooled or superheated) states becomes necessary also when disorder broadens a FOPT, because the discontinuities (in entropy and magnetisation) are now smudged out and cannot be measured.

In this article we shall present our studies on two classes of systems where disorder influences a FOPT. The first one is the vortex matter in hard superconductors (i.e. type-II superconductor with finite critical current J_C) where one can observe FOPT involving vortex solid–solid as well as vortex solid–liquid phases. Inside hard type-II superconductor samples vortex pinning causes local variation in H. Since H is varying within the sample, and since vortex matter transition temperature T_C varies with H, different regions of the sample will be at the transition point for different values of applied H. The FOPT thus occurs, in different regions of the sample, at different values of T, and the FOPT is completed over a broad range of temperature. We shall discuss our experimental results on a vortex matter solid–solid phase transition in some hard superconductors.

The second class of systems will be doped magnetic materials, which show a first-order ferromagnetic to antiferromagnetic transition as either temperature or field is varied. In this family the disorder is because of doping, where the intrinsic disorderly (or random) distribution of dopants causes a distribution in the near-neighbour exchange interactions, and thus in the temperature (or field) at which the transition would occur. We shall discuss our results on a broad FOPT in doped $CeFe_2$.

Downloaded At: 12:30 28 January 2011

2. FIRST-ORDER PHASE TRANSITION: PHENOMENOLOGY

The standard treatment of phenomenology of a first-order transition (Chaikin and Lubensky, 1995; Chaddah and Roy, 2000) considers that only T is varied while another possible control variable like H is held constant. The free-energy density is expressed in terms of the order parameter S as

$$f(T,S) = (r/2)S^2 - wS^3 + uS^4, \tag{1}$$

where w and u are positive and temperature independent (Chaikin and Lubensky, 1995). We will assume here that symmetry does not prohibit terms of odd order. If it does, then the free energy would be expressed as $f = (r/2)S^2 - wS^4 + uS^6$, and it is easy to follow and carry through all subsequent arguments. The assumption of the form of Eq. (1) is thus made without loss of generality. At $T = T_C$ the two stable states with $f = 0$ are at $S = 0$ and at $S = S_C = w/(2u)$. These are separated by an energy barrier peaking at $S = S_B = w/(4u)$, of height $f_B = w^4/256\,u^3$. These results are independent of any assumption about the detailed T dependence of $r(T)$. The standard treatment (Chaikin and Lubensky 1995) assumes that $r(T) = a[T - T^*]$, where a is positive and T independent, and where d^2f/dS^2 at $S = 0$ vanishes at $T = T^*$. Simple algebra shows that the limit of metastability on cooling is reached at $T^* = T_C - w^2/2\,ua$. Similarly the limit of metastability on heating is reached at $T^{**} = T_C + w^2/16\,ua$. Supercooling (or superheating) can persist till T^* (or T^{**}) only in the limit of infinitesimal fluctuations. The barrier height around $S = 0$ drops continuously as T is lowered

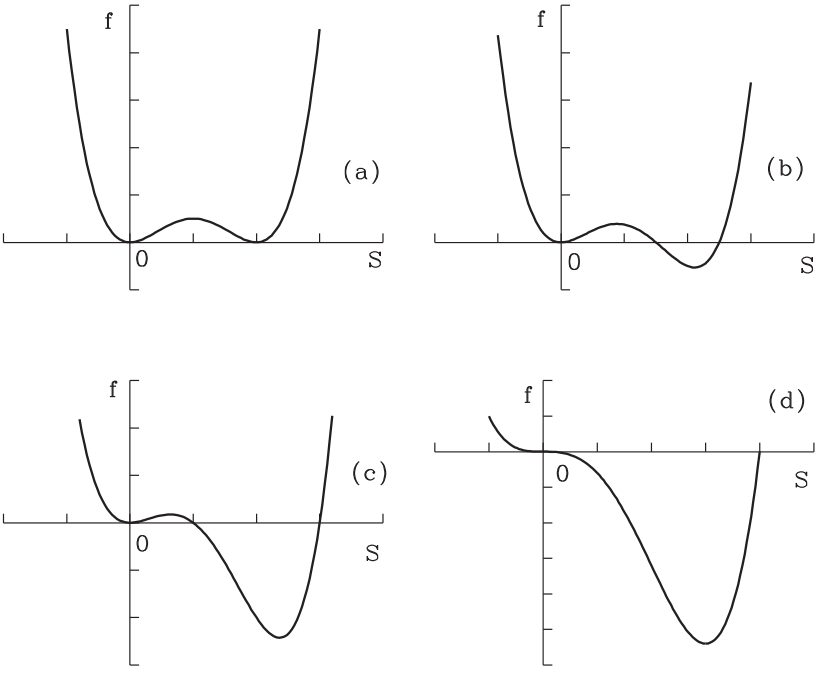

FIGURE 1 Schematic free-energy curves for (a) $T = T_C$, (b) $T = T_1 < T_C$, (c) $T = T_2 < T_1$ and (d) $T = T^*$. The higher temperature phase sits in a local minimum and is stable against infinitesimal fluctuations for $T_C > T > T^*$. This local minimum becomes shallower as T is lowered below T_C and the disordered state at T_2 is unstable to a smaller fluctuation energy than at T_1 (Chaddah and Roy, 2000).

Downloaded At: 12:30 28 January 2011

below T_C, and this is depicted in Fig. 1. In the presence of a fluctuation of energy e_f, supercooling will terminate at T_O where the energy barrier satisfies

$$f_B(T_O) \approx [e_f + k_B T_O]. \tag{2}$$

Similarly, the barrier height around the ordered state drops continuously to zero as T is raised towards T^{**}, and this is depicted in Fig. 2. The fluctuation energy in the ordered state will dictate when superheating will terminate.

The formulation stated above is of course valid for a FOPT in vortex matter and magnetic systems (to be described below) as a function of T. However, phase transitions in these systems in general are encountered in H,T phase-space, and the limit of supercooling (T^*) and superheating (T^{**}) is now a function of H (Chaddah and Roy, 2000). It is quite instructive to have a schematic phase diagram (see Fig. 3) showing the phase transition line and the metastable region associated with it, and this will be useful in discussing various experimental results to be presented in the subsequent section. For the sake of clarity we do not show the limit of metastability while heating in this schematic (H,T) phase diagram, and the various arguments put forward for supercooling will hold for superheating as well.

In addition the presence of disorder will reduce the barrier height locally at the site of disorder, and these sites will act as nucleation centres for the stable phase. This in turn will introduce phase coexistence of stable and metastable phases in the T-regime

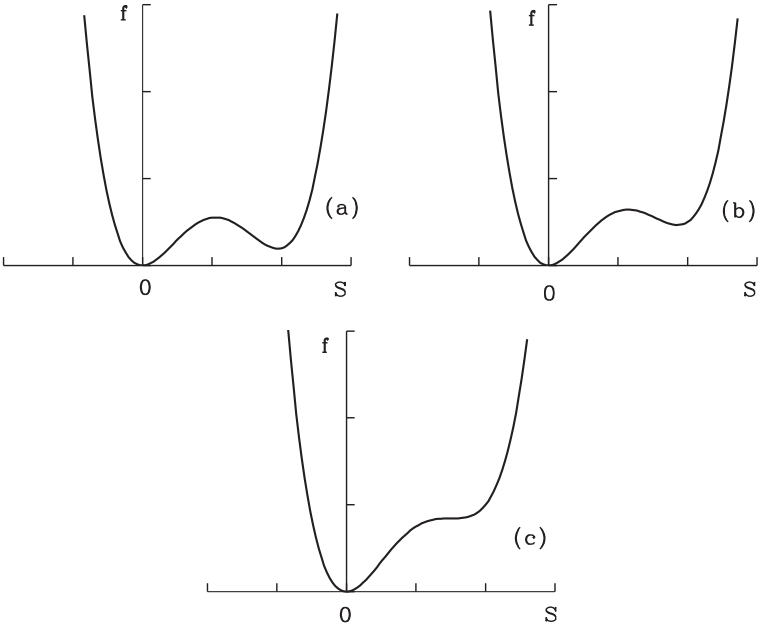

FIGURE 2 Schematic free-energy curves for (a) $T = T_3 > T_C$, (b) $T = T_4 > T_3$ and (c) $T = T^{**}$. The lower temperature phase sits in a local minimum and is stable against infinitesimal fluctuations for $T_C < T < T^{**}$ (Chaddah and Roy, 2000).

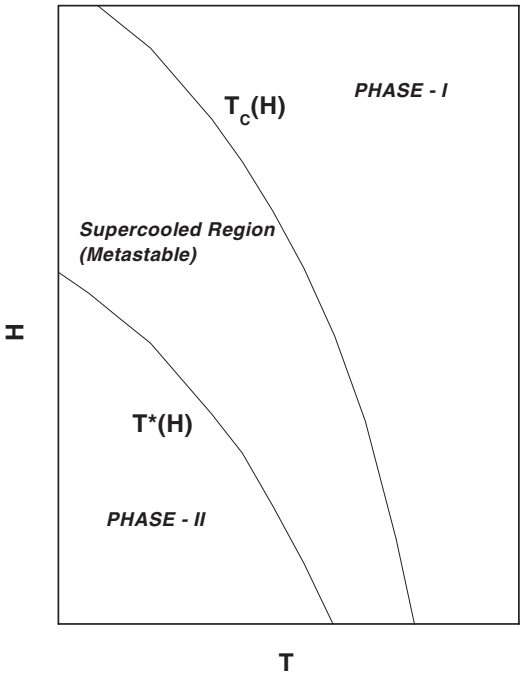

FIGURE 3 Schematic (H,T) phase diagram showing the phase transition line $T_C(H)$ and the stability limit $T^*(H)$ for the supercooled state. The H–T regime between $T_C(H)$ and $T^*(H)$ while cooling is the supercooled regime.

Downloaded At: 12:30 28 January 2011

$|T_C - T^*|$ (or T^{**}). Such phase coexistence, of course, is highly metastable in nature, and any kind of energy fluctuation readily increases the volume fraction of the stable phase. Further, random quenched impurities under certain circumstances produce a landscape of FOPT in the sample due to local fluctuations in thermodynamic phase. According to Imry and Wortis (1979) such fluctuations occur when the free energy lowering (because local fluctuations in impurity density are taken advantage of), more than offsets the free-energy cost of the interface produced. Macroscopically, in such a situation the FOPT line in the H–T phase diagram of a given sample will be replaced by a distribution of FOPT lines, i.e. a FOPT band. This in turn will lead to a band of $T^*(H)$ and $T^{**}(H)$.

As noted earlier the experimental indication of a first-order transition usually comes via a hysteretic behaviour of various properties, not necessarily thermodynamic properties. As an example, the first indication of a first-order melting transition from elastic solid to vortex liquid in a vortex matter came via distinct hysteresis observed in transport property measurements (Safar *et al.*, 1992). The confirmatory tests of the first-order nature of a transition, of course, involve the detection of discontinuous change in thermodynamic observable and the estimation of latent heat. There also exists a less rigorous class of experimental tests, which involves the study of phase inhomogeneity and phase coexistence across a FOPT. These experiments are relatively easy to perform, especially in comparison to measuring of latent heat, and become quite effective in situations where latent heat is small and difficult to distinguish experimentally (White and Geballe, 1979). This is particularly so in the case of disorder influenced FOPT, and in subsequent sections we shall show the usefulness of hysteresis and phase coexistence in the study of such transitions in vortex matter and magnetic systems.

Downloaded At: 12:30 28 January 2011

3. FIRST-ORDER VORTEX SOLID–SOLID TRANSITION IN VORTEX MATTER OF TYPE-II SUPERCONDUCTORS

Since the discovery of high-T_C superconductors (HTSC), the physics of the vortex lattice of type-II superconductors has come under much scrutiny especially due to the technological importance of critical current J_C, which depends on the pinning properties of vortices (Blatter *et al.*, 1994). The H–T phase diagram of the flux-line lattice of various type-II superconductors – both high T_C and low T_C – has been studied in detail, and the subject of flux-line lattice in the presence of pinning and thermal fluctuations is now known as vortex matter (Blatter, 1997). One of the interesting aspects of vortex matter is the possible transition from a low-T low-H quasi-ordered vortex solid or Bragg-glass to a low-T high-H disordered vortex solid or vortex glass (Vinokur *et al.*, 1998). The general consensus now is that this transition is first order in nature (Vinokur *et al.*, 1998; Paltiel *et al.*, 2000; Avraham *et al.*, 2001; Radzyner *et al.*, 2002), and this was actually established experimentally first in a low-T_C superconductor $CeRu_2$ (Roy and Chaddah, 1997). The general features of this vortex solid–solid transition in bulk magnetic and transport properties are described below.

Figure 4 shows the M versus H plot of $CeRu_2$ ($T_C \approx 6.2$ K) representing the magnetic response of the vortex matter of the sample at 4.5 K (Roy *et al.*, 2000b). The irreversibility of the M arises due to the pinning of the flux-line lattice and it is a general property of the type-II superconductors with pinning. This irreversible magnetisation (M_{irrv})

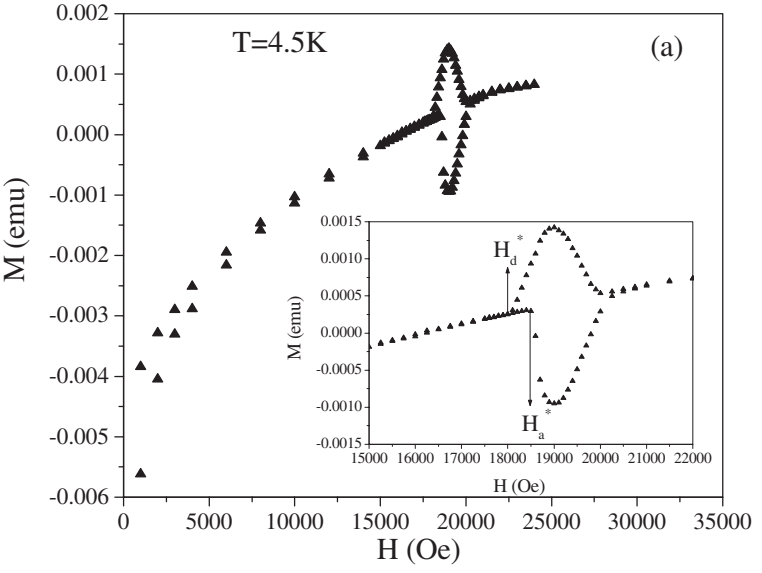

FIGURE 4 Magnetization (M) vs. field (H) plot for $CeRu_2$ at 4.5 K. The insets highlight the peak-effect regime (Roy *et al.*, 2000b).

Downloaded At: 12:30 28 January 2011

is correlated to the J_C of the sample, and this decreases as a function of H and goes to zero at a characteristic field $H_{\text{irrev}} \leq H_{C2}$, where H_{C2} stands for the upper critical field. The indication of the vortex solid–solid transition comes from the field-induced enhancement of the M_{irrv} or J_C before going to zero at H_{irrev}. This phenomenon, commonly known as the 'peak-effect', has actually been reported in various low-T_C superconductors (Chaudhary *et al.*, 2000b) well before the arrival of HTSC materials and has been attributed initially to flux-line lattice softening (Pippard, 1969). This is now a common feature in all HTSC materials and is the subject of much scrutiny. We now show that the onset of the enhanced M_{irrv} or J_C is accompanied by hysteresis and metastability typical of a FOPT process. It should be noted here that the observables – M_{irrv} and J_C – are metastable properties themselves. So extra caution is necessary here to distinguish the hysteresis and metastability arising from the FOPT process, since in true sense we shall be dealing with 'hysteresis of hysteresis'.

The M–H curve in Fig. 4 is obtained by zero-field cooling to 4.5 K and then raising H isothermally to 50 kOe and then cycling H under same isothermal condition between 50 and −50 kOe. The master M–H curve thus obtained shall be termed as 'envelope curve'. The 'peak effect' (PE) regime (highlighted in the inset of Fig. 4) is separated from the usual irreversible M–H behaviour by a H-regime where magnetisation is (almost) reversible in nature. The onset field of the PE in the ascending H-cycle is distinctly different from that in the descending H-cycle, and this is particularly distinct for the single crystal samples (Roy *et al.*, 2000b). Such hysteresis is necessarily a signature of a FOPT. We have developed a 'minor hysteresis loop (MHL)' technique (Roy and Chaddah, 1997) to highlight this FOPT process further and to distinguish 'hysteresis of hysteresis' from the commonly encountered 'M_{irrv}' in vortex matter. One can draw MHL from any point on the envelope curve just by reversing the field direction from that point. The characteristic behaviour of the MHLs, which are contained

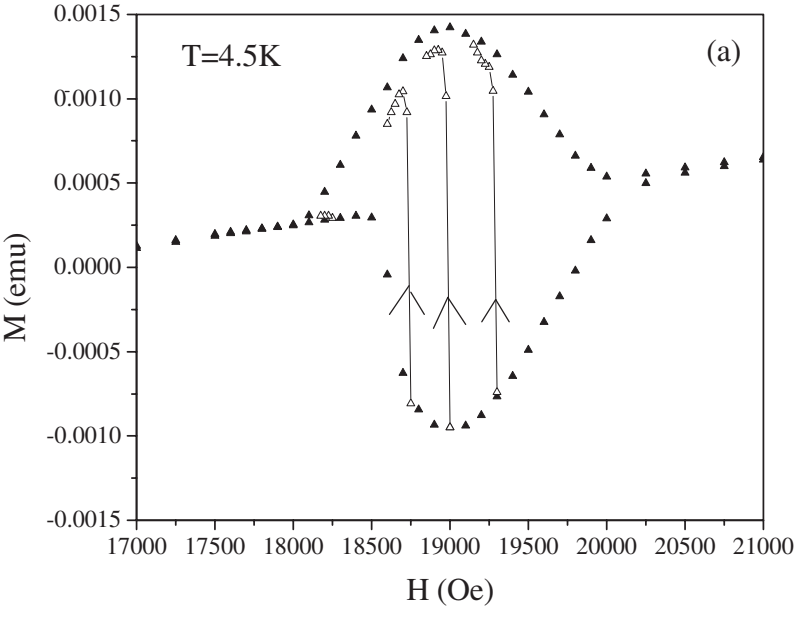

FIGURE 5 Forward legs of minor hysteresis loops (MHL) at 4.5 K initiated from the lower envelope M–H curve at $H = 18.25$, 18.75 and 19 kOe; they saturate without touching the upper envelope curve. MHL initiated from 19.6 kOe saturates on touching the upper envelope curve (Roy *et al.*, 2000b).

Downloaded At: 12:30 28 January 2011

within the envelope curve of an usual hard type-II superconductor is well documented (Chaddah *et al.*, 1992). These MHLs saturate touching the envelope curve (opposite to the one from which the MHLs are generated) once the change in applied H is greater than the field for full penetration of the sample (Roy and Chaddah, 1997). This expected behaviour of MHLs has been observed in the $CeRu_2$ samples in the field region away from the onset of PE regime. However, there is a drastic change in behaviour of the MHLs at the onset of the PE regime. In the ascending H-cycle the MHLs saturate without touching the envelope curve, and in the descending H-cycle they overshoot the lower envelope curve (see Fig. 5). As discussed in detail in Roy and Chaddah (1997) these MHLs actually track the nucleation and growth of the higher (lower) field vortex state in the ascending (descending) H-cycle and help to establish the region of superheating (supercooling). The usefulness of MHLs in such studies will be more apparent in the study of magnetic systems (described in the next section) where the observable is an equilibrium property. The metastable behaviour associated with the first-order vortex solid–solid transition in $CeRu_2$ is highlighted by the marked field-sweep-rate dependence of magnetisation in the respective field regime (Roy *et al.*, 1999) and large magnetic relaxation (Chattopadhyay *et al.*). The conjecture of the first-order vortex solid–solid transition is further supported by transport properties measurements (Chaudhary *et al.*, 2000a). It has been shown that the extent of the supercooled region is more in the field cooling measurements across the transition point (Roy *et al.*, 1998b, 1999, 2000b). This is amply supported by the argument that the energy fluctuations associated in the magnetic field variation along an isothermal path drive the metastable state to the stable state, thus limiting the extent of supercooling (Chaddah and Roy, 1999, 2000). The width of the transition seemingly depends on

the disorder profile of the sample as evidenced from the study of polycrystalline samples of $CeRu_2$ of various purity and doping (Roy and Chaddah, 1997, 1999; Roy *et al.*, 1998a) and single-crystalline samples (Roy *et al.*, 2000b). This will imply the importance of intrinsic quenched-disorder induced landscape of transition field/temperature (Imry and Wortis, 1979) in addition to the field variation within the sample due to the finite demagnetisation factor and J_C. This matter has already been discussed in detail in the context of the melting of vortex solid (Soibel *et al.*, 2000).

The same MHL technique has now been used to study the vortex solid–solid transition in $NbSe_2$ (Ravikumar *et al.*, 1999), V_3Si (Kupfer *et al.*, 2003), MgB_2 (Angst *et al.*, 2003), YBaCuO (Radzyner *et al.*, 2000; Zhukov *et al.*, 2001). A general consensus now seems to be emerging on the first-order nature of this transition, with additional studies involving various other experimental techniques in both high-T_C (Giller *et al.*, 2000) and low-T_C materials (Ling *et al.*, 2001).

4. FIRST-ORDER FERROMAGNETIC TO ANTIFERROMAGNETIC TRANSITION IN MAGNETIC SOLIDS

Downloaded At: 12:30 28 January 2011

First-order ferromagnetic (FM) to antiferromagnetic (AFM) transition as a function of T and H is quite common in magnetic solids and seems to be playing an important role in the functionality of at least two classes of novel materials of current interest namely manganese-oxide systems showing colossal magnetoresistance (CMR) (Dagotto *et al.*, 2001) and giant magnetocaloric materials (Pecharsky *et al.,* 2003). Phase coexistence and metastability are the common features in these disparate classes of magnetic materials, and this commonality has largely gone unnoticed so far. Here we use a relatively simple magnetic system, namely doped-$CeFe_2$ alloys as a test-bed materials system to study a first-order FM–AFM transition in detail. We show clear evidence of magnetic phase coexistence and metastability as the system is driven across the entire first-order FM–AFM transition as a function of T and H. We argue that the phase coexistence and metastability arise as natural consequence of an intrinsic disorder-influenced first-order transition.

$CeFe_2$ is a cubic Laves phase ferromagnet (with Curie temperature $\approx$230 K) (Paolisini *et al.*, 1998), where small substitution ($<10\%$) of selected elements such as Co, Al, Ru, Ir, Os and Re can induce a low-temperature AFM state with higher resistivity than the FM state (Roy and Coles, 1989). A giant magnetoresistance effect (Kunkel *et al.*, 1996) associated with the AFM–FM transition is well documented. Neutron diffraction studies on these doped-$CeFe_2$ samples revealed a discontinuous change of the unit cell volume at the FM–AFM transition, confirming that it is first order (Kennedy and Coles, 1990). We have used these well-characterised Al, Ru and Ir-doped $CeFe_2$ alloys for our study of FOPT. The preparation and characterisation of these polycrystalline alloys have been described in detail in Roy and Coles (1989) and Kennedy and Coles (1990).

Figure 6 shows the ac-susceptibility (χ) for a 5% Ir-doped and a 7% Ru-doped $CeFe_2$ sample as a function of T (Manekar *et al.*, 2000a). The paramagnetic (PM) to FM transition is characterised by a sharp increase in susceptibility (χ) with the decrease in T. The transition occurs at $T_{\text{Curie}} \approx 185$ K in the 5% Ir-doped sample, and $T_{\text{Curie}} \approx 165$ K in the 7% Ru-doped sample. Below T_{Curie}, susceptibility more or less flattens out for both the samples, before decreasing sharply at around 135 K in 5%

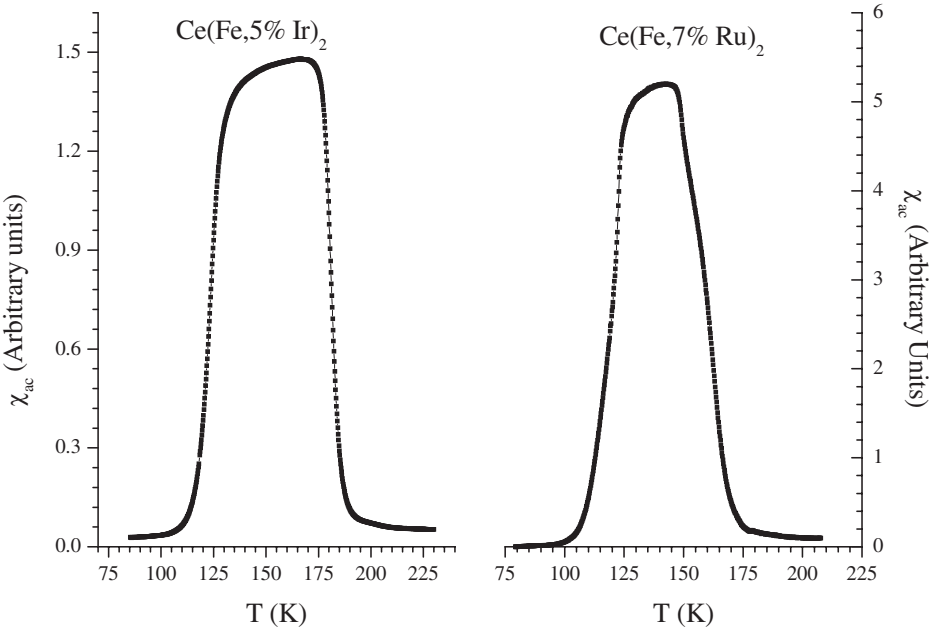

FIGURE 6 AC susceptibility (χ) vs. temperature (T) plots for (a) $Ce(Fe, 5\%\ Ir)_2$ (b) $Ce(Fe, 7\%\ Ru)_2$ (Manekar *et al.*, 2000a).

Downloaded At: 12:30 28 January 2011

Ir-doped $CeFe_2$, and at around 125 K in 7% Ru-doped $CeFe_2$. This low-temperature decrease in $\chi(T)$ marks the onset of FM–AFM transition at a temperature T_N. There is no effect of thermal cycling on the PM–FM transition of either of these samples and this is in consonance with the second order-nature of this transition (Manekar *et al.*, 2000a). Within the same experimental resolution, however, distinct thermal hysteresis is observed across the FM–AFM transition (see Fig. 7). This is necessarily a signature of a FOPT.

To study the phase coexistence we use the MHL technique described earlier in the context of vortex matter phase transition. We first define the 'envelope curve' as the curve enclosing the thermally hysteretic susceptibility between the lower and higher temperature reversible region (see Fig. 7). We can draw a MHL during the heating cycle, i.e. start heating and increase T from the lower temperature reversible (AFM) region and then reverse the direction of T before reaching the higher T reversible (FM) region. We can also draw a MHL in the cooling cycle i.e. start cooling from the reversible FM region and reverse the direction of T before reaching the lower T reversible AFM region. If the heating is reversed at sufficiently 'low' T the minor loop does not coincide with the cooling part of the 'envelope curve'. Here in the lower part of the hysteretic regime the high-T FM phase is not formed in a sufficient quantity; so when T is decreased the curve does not fall on the cooling part of the envelope curve, which represents the curve along which the high-T phase is supercooled. The MHLs initiated from T well inside the hysteretic regime coincide with the cooling part of envelope curve indicating that the high-T phase has formed in a sufficient quantity. In Figs. 8 and 9 we present some representative MHLs both for the 5% Ir-doped $CeFe_2$ and 7% Ru-doped $CeFe_2$ alloys. This behaviour of MHLs is reproduced over many experimental cycles. The presence of these MHLs clearly suggests the existence of

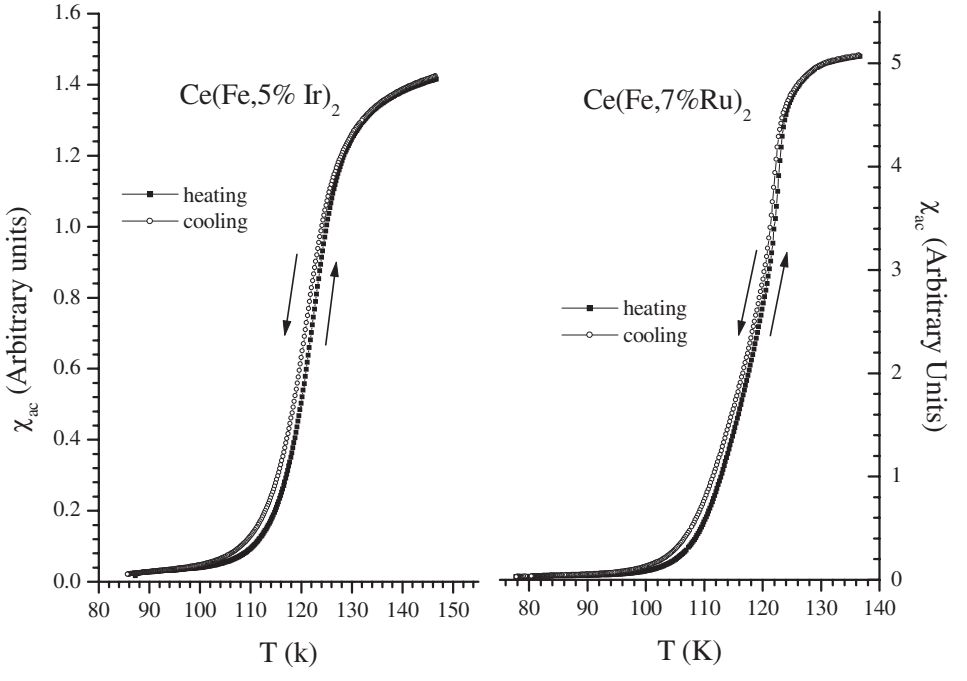

FIGURE 7 χ vs. T plot highlighting the thermal irreversibility of the FM–AFM transition in Ce(Fe, 5% Ir)$_2$ and Ce(Fe, 7% Ru)$_2$ (Manekar *et al.*, 2000a).

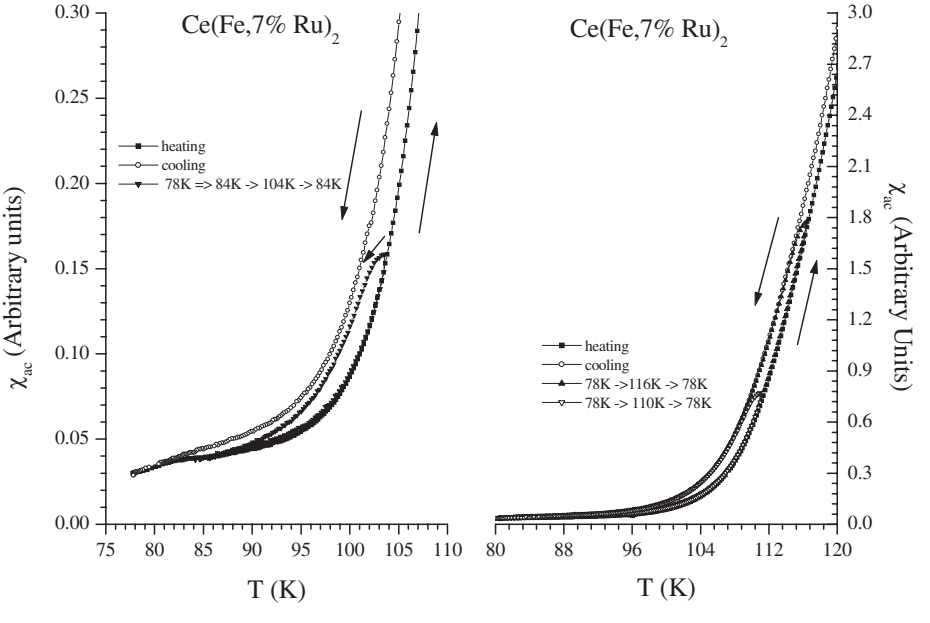

FIGURE 8 Minor hysteresis loops (MHL) in χ vs. T plot highlighting phase coexistence in Ce(Fe, 7% Ru)$_2$: representative MHL initiated from the lower part of the hysteretic regime (left), and representative MHLs initiated from well inside the hysteretic regime (right) (Manekar *et al.*, 2000a).

Downloaded At: 12:30 28 January 2011

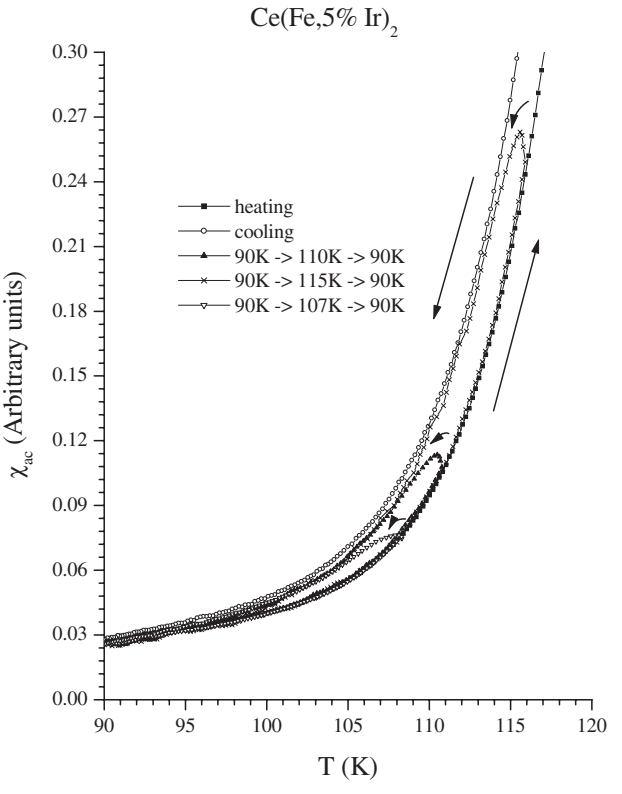

FIGURE 9 Minor hysteresis loops (MHL) in χ vs. T plot highlighting phase coexistence in Ce(Fe, 5% Ir)$_2$ (Manekar *et al.*, 2000a).

Downloaded At: 12:30 28 January 2011

phase coexistence across the FM–AFM transition (Manekar *et al.*, 2000a). The same kind of experiments can be performed using other experimental measured quantities like dc magnetisation and resistivity as observable.

In the low-temperature AFM regime a transition from the zero field AFM state to FM state can be induced by application of an H (Manekar *et al.*, 2000b). In dc magnetisation study this field-induced AFM–FM transition is marked by a sharp rise in M. We mark the onset field of this metamagnetic transition as H_M. Focusing on this metamagnetic transition, we shall now identify signatures typically associated with a first-order phase transition, namely hysteresis and phase coexistence. We present in Figs. 10 and 11 M–H curves obtained in the ascending and descending H-cycles for both for 5% Ir-doped $CeFe_2$ and 7% Ru-doped $CeFe_2$ samples, showing distinct hysteresis associated with the metamagnetic transition. A sharp rise in M accompanied by hysteresis is traditionally attributed to the first-order magnetic process (Bean and Rodbell, 1962). However, it can still be argued that the observed hysteresis may be the intrinsic property of the field-induced FM state and originates from the domain wall pinning and/or freezing of domain rotation. To negate these possibilities we have carefully measured the M–H curves for both the samples in the T-regime where the ground state is FM at all H values. M–H curves in the FM regime reveal a negligibly small hysteresis with the coercivity field (H_C) of the order of 5 Oe which does not change appreciably with T. In contrast the hysteresis associated with the metamagnetic

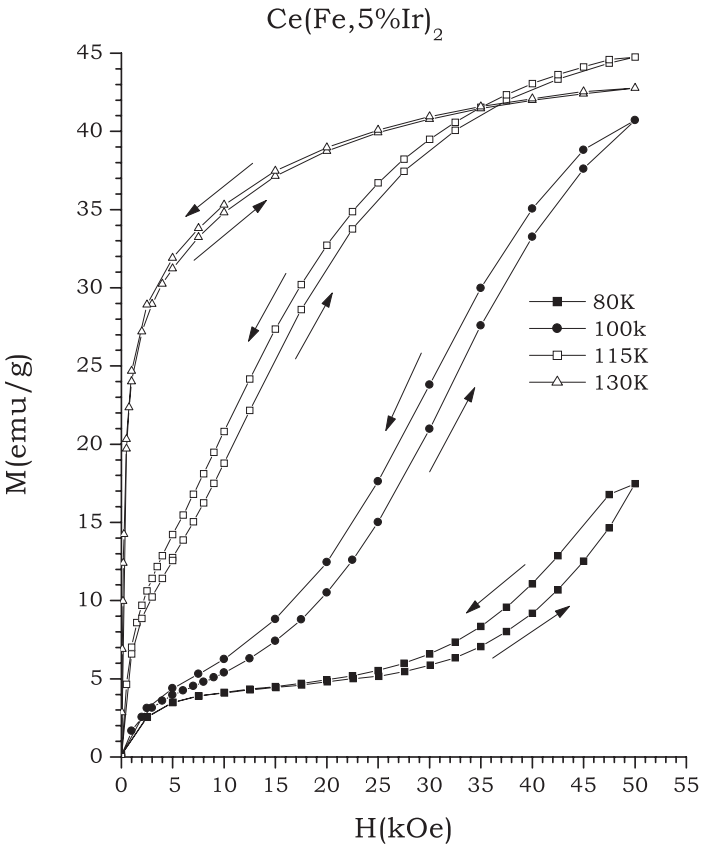

FIGURE 10 M–H curves for Ce(Fe, 5% Ir)$_2$ showing hysteresis associated with the metamagnetic transition. The arrows show the direction of field change (Manekar *et al.*, 2000b).

Downloaded At: 12:30 28 January 2011

transition shows up as a distinct bubble in an intermediate H-regime, with reversibility above and below (see Fig. 6 of Manekar *et al.* (2001b)). The size of this hysteresis bubble grows rapidly with the decrease in T below T_N.

Having established the hysteretic nature of the metamagnetic transition, we shall now look for the phase coexistence in the transition region using the MHL technique. We shall first define the hysteretic M–H curve obtained by isothermal field cycling between 0 and $H_{\max}$ as the 'envelope curve'. We can now generate an MHL during the ascending H-cycle, i.e. start increasing H from the lower field reversible (AFM) regime and then reverse the direction of H before reaching the higher field saturation magnetisation regime (Manekar *et al.*, 2000b). We can also produce an MHL in the descending H-cycle, i.e. start decreasing H from the saturation magnetisation regime and reverse the direction of H before reaching the low-H AFM regime. We show in Figs. 12 and 13 examples of these MHLs in 5% Ir-doped $CeFe_2$ and 7% Ru-doped $CeFe_2$ samples. In the ascending H-cycle, if the MHL is initiated at H values not well above H_M the MHL does not touch the descending field or upper envelope curve (see Figs. 12 and 13). Here in the lower part of the hysteretic regime, the high-field FM phase is not formed in sufficient quantities; so when H is decreased the MHL does not touch the descending part of the envelope curve which actually represents the path along

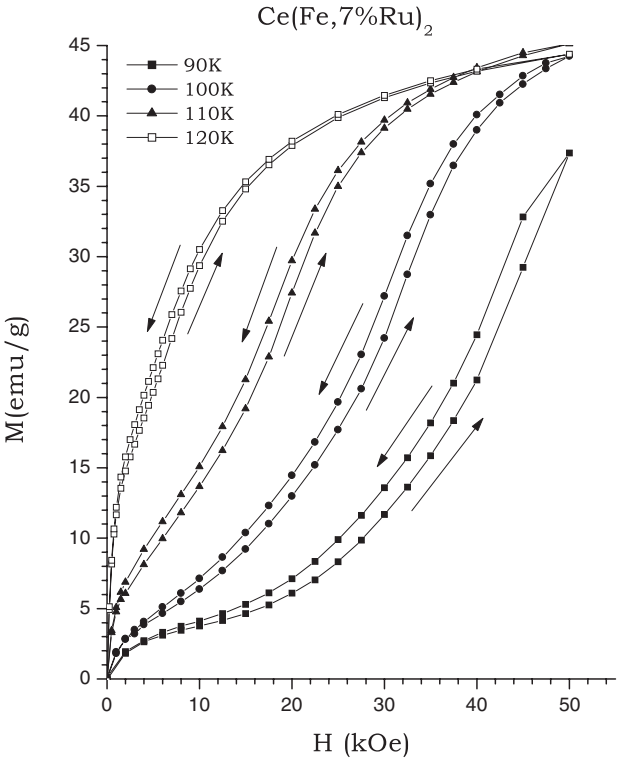

FIGURE 11 M–H curves for Ce(Fe, 7% Ru)$_2$ showing hysteresis associated with the metamagnetic transition. The arrows show the direction of field change (Manekar *et al.*, 2000b).

Downloaded At: 12:30 28 January 2011

which the field-induced FM phase is supercooled. The MHLs initiated from H values well inside the hysteretic regime coincide with the upper envelope curve (see Figs. 12 and 13), indicating that the high-field FM phase has formed in sufficient quantities. To show further evidence of supercooling of the high-field phase, in Fig. 14 we show MHLs at $H = 2$ kOe drawn from the lower envelope curve and at $H = 1.6$ kOe drawn from the upper envelope curve of the 7% Ru-doped $CeFe_2$ sample. These field values are chosen such that the lower and upper envelope curve has the same M value. Note that $H = 2$ kOe is lower than the estimated H_M, and accordingly the MHL drawn from the lower envelope curve shows almost no irreversibility. However, the MHL drawn from the upper envelope curve at a lower H value of 1.6 kOe shows distinct irreversibility. This clearly shows that the high-field phase persists in this field regime in the descending H-cycle.

We shall now highlight the presence of interesting memory effects across the FM–AFM transition. Figure 15 shows a M versus T plot for a 4% Ru-doped $CeFe_2$ sample in an applied field of 20 kOe. Three different measurement protocols were used: zero-field cooled (ZFC), field-cooled cooling (FCC) and field-cooled warming (FCW). The PM–FM transition is marked by the rapid rise of M with decreasing T below $\sim$210 K and it is thermally reversible. The FM–AFM transition is marked by the sharp drop in M below 50 K and shows substantial thermal hysteresis, which is necessarily a signature of FOPT. It should be noted that the FCC curve does not merge with the ZFC curve down to the lowest measured temperature of 5 K. We

have obtained similar M–T curves for applied fields between 100 Oe and 30 kOe. Thermal hysteresis is always present in the AFM–FM transition, and broadens with increasing field, so that when the applied field $H \geq 15$ kOe the M_{FCC} (T) and M_{ZFC} (T) curves fail to merge. $M_{ZFC} \neq M_{FC}$ is an essential feature of the spin-glasses below the spin-glass transition temperature and is termed thermomagnetic irreversibility (TMI). However, unlike in the present case the TMI in spin-glasses collapse with the increase in applied H. Further it will be shown below that in contrast with the equilibrium field cooled state of spin-glass, here the field cooled state below the transition is a metastable state. A very similar increase in TMI with an applied field has been observed across FM–AFM transition in CMR Mn-oxide systems (Freitas *et al.*, 2002). Figure 16 shows the schematic H–T phase diagram based on our magnetisation measurements with $T_{NW}(T_{NC})$ as the temperature of the sharp rise (fall) in M in the ZFC (FCC)

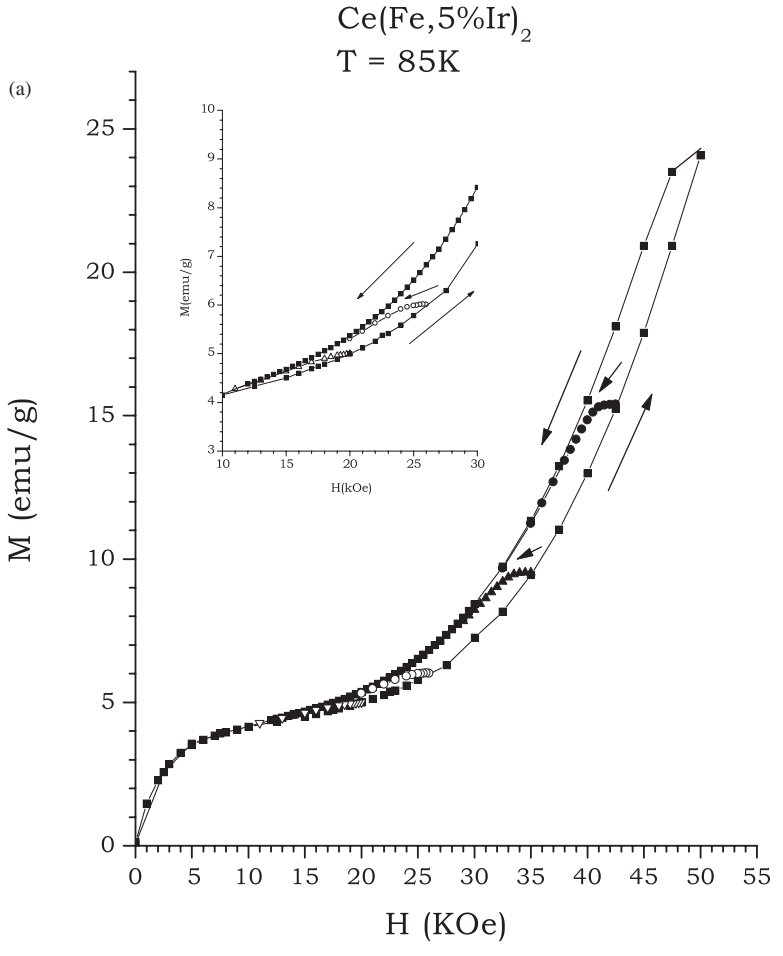

FIGURE 12 Minor hysteresis loops generated during: (a) ascending H-cycle for $Ce(Fe, 5\%\ Ir)_2$ at $H = 20$ kOe (open triangle), $H = 26$ kOe (open circle), $H = 35$ kOe (solid triangle) and $H = 42.5$ kOe (solid circle); (b) descending H-cycle for $Ce(Fe, 5\%\ Ir)_2$ at $H = 40$ kOe (open square) and $H = 45$ kOe (solid triangle). The envelope curve is represented by solid squares. The measurements were done at $T = 85$ K. Inset shows the expanded view (Manekar *et al.*, 2000b).

Downloaded At: 12:30 28 January 2011

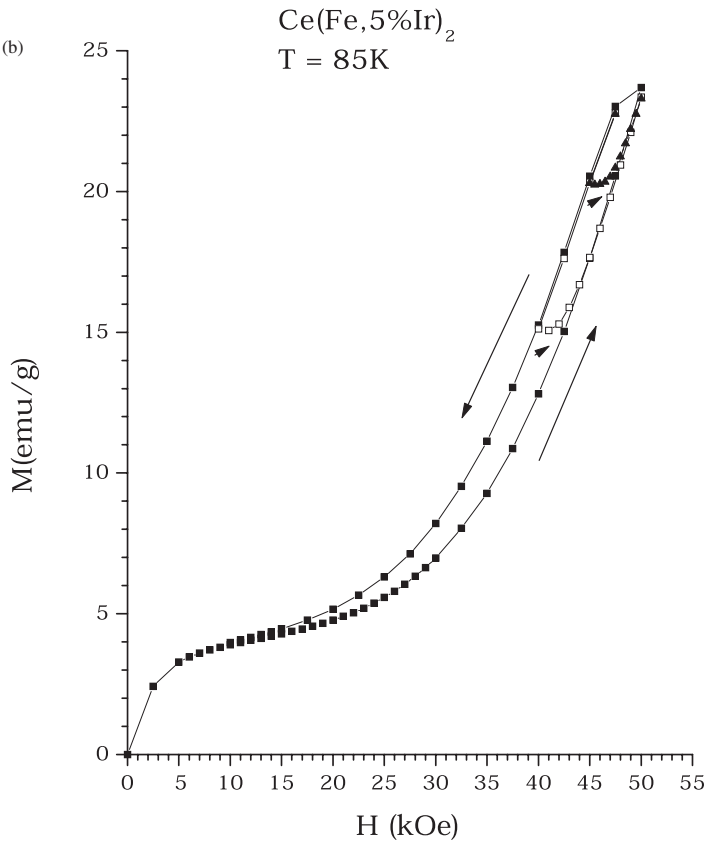

FIGURE 12 Continued.

Downloaded At: 12:30 28 January 2011

cycle (see inset of Fig. 16). T_{NC} is more closely defined as the temperature where dM/dT in the M versus T plot changes sign from negative to positive. T^* is the low-T point where M_{ZFC} and M_{FC} merges and T^{**} is the high-T counterpart. T^{**} and T_{NC} appear almost the same in our present magnetisation measurements, but can be distinguished clearly in resistivity measurements under same experimental protocol. Note that T_{NW} $(H) < T_{NC}$ (H), i.e. the onset of nucleation of the AFM state on cooling occurs at a higher temperature than does nucleation of the FM phase during warming; this indicates that we are dealing with a disorder-broadened first-order transition. The disorder-influenced broadening is observed in the sample in the field-induced transition also, and this is discussed in detail in Chattopadhyay *et al.* (2003).

From Fig. 16 it is quite clear here that it is possible to retain a residual FM state in this 4% Ru-doped $CeFe_2$ alloy down to the lowest T of measurements by following the FCC path with applied $H \geq 15$ kOe. This is exactly what is known as field annealing of the FM state in various CMR Mn-oxide systems (Kimura *et al.*, 1999). We shall now show that the magnetic state with residual FM state obtained by this FCC path is actually metastable in nature. First we draw an isothermal M–H curve in the ZFC state at 5 K by field cycling between 0 and 30 kOe. A distinct 'end point memory' is observed for this M–H curve; namely on completion of the field cycles, the same end point magnetisation value is obtained at 30 kOe (see Fig. 17). This clearly shows that the magnetic

state is stable with respect to any field cycling. However, the isothermal M–H curve obtained after field cooling to 5 K in a field of 30 kOe shows a distinct lack of 'end point memory' just after a small cycle of reducing the field to 20 kOe and back to 30 kOe (see Fig. 17). The difference in the end point magnetisation increases with the successive field cycling with increasing amplitude and reaches a maximum value after a complete cycle to 0 Oe and back to 30 kOe. Any subsequent field excursion, however, retains the 'end point memory'. This clearly shows that the residual FM obtained by the FCC path is very much metastable in nature and can be erased by field cycling. This kind of behaviour is in striking contrast with the nonequilibrium behaviour of spin-glasses, hard ferromagnets and hard superconductors, where the magnetisation hysteresis loops always show 'end point memory'.

All these observations can be rationalised in terms of supercooling of the FM state. While cooling across the first-order FM–AFM transition, some amount of the FM state will supercool into the T-regime well below the transition line. The extent of the T-regime of supercooling actually widens in the presence of the applied magnetic field, and as mentioned earlier in the context of vortex matter, the extent of supercool-

Downloaded At: 12:30 28 January 2011

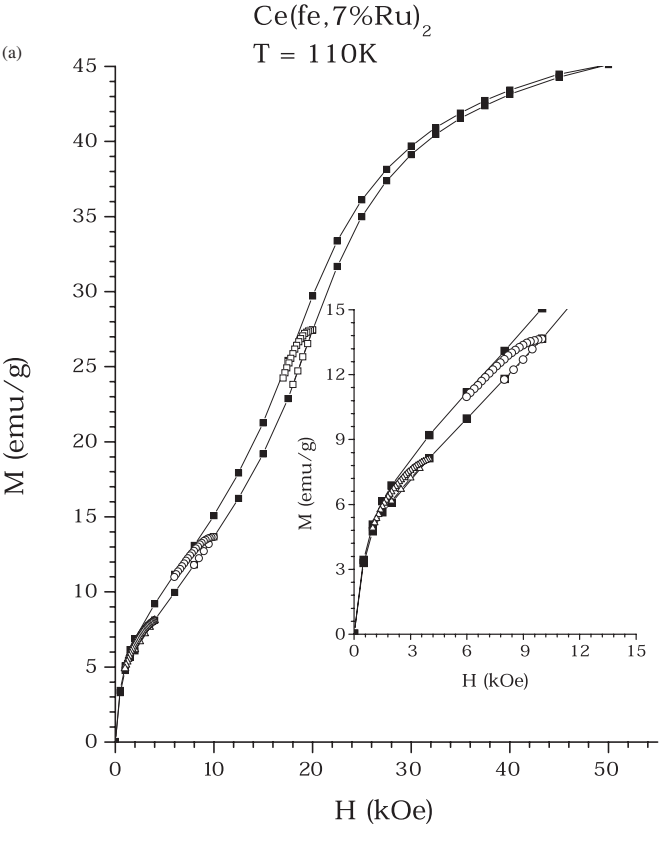

FIGURE 13 Minor hysteresis loops generated during (a) the ascending H-cycle for Ce(Fe, 7% Ru)$_2$ at $H = 4$ kOe (open triangle), $H = 10$ kOe (open circle) and $H = 20$ kOe (open square); (b) descending H-cycle for Ce(Fe, 7% Ru)$_2$ at $H = 8$ k Oe (open square) and $H = 22$ kOe (open circle). The envelope curve is represented by solid squares. The measurements were done at $T = 110$ K. The inset shows the expanded view (Manekar *et al.*, 2000b).

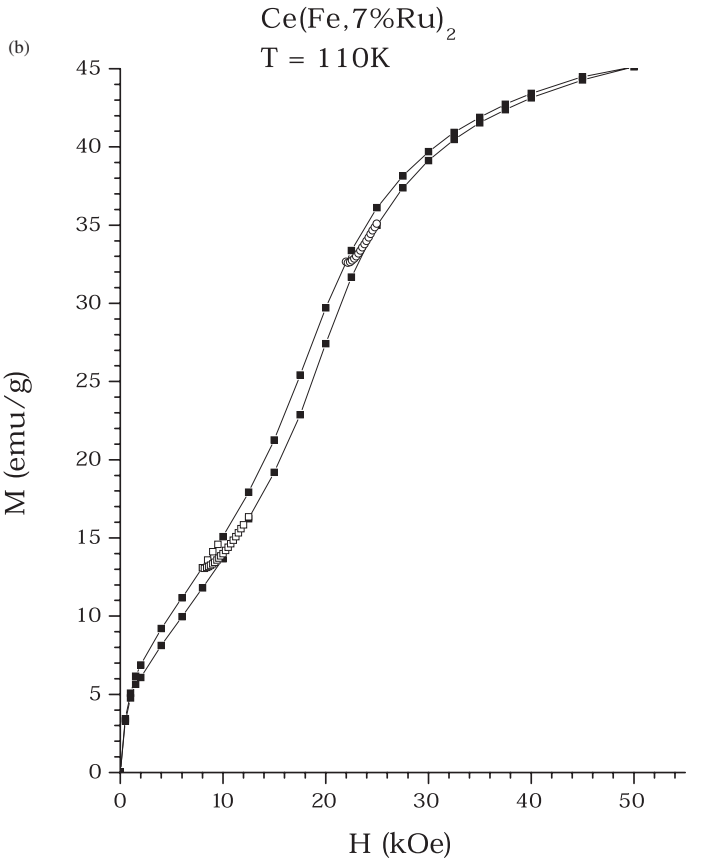

FIGURE 13 Continued.

Downloaded At: 12:30 28 January 2011

ing is more while following an FCC path (see Roy *et al*., 1998a). It is clear from Fig. 16 that with applied $H < 15$ kOe the supercooled FM state will cease to exist below a finite T, and one can reach the stable AFM state. This is indicated by the merger of the FC and ZFC magnetisation. With $H \geq 15$ kOe some amount of supercooled FM state remains down to the lowest T of measurement. As a result FC magnetisation always remains higher than the ZFC counterpart in the temperature regime below the FM–AFM transition. The region between $T_{NC}(H)$ and $T^*(H)$ line in Fig. 16 marks the phase-coexistence region formed during the cooling path. At the onset of the FM–AFM transition, the regions with AFM ordering will start nucleating, and the nucleation will be complete at the $T^*(H)$ line. The phase-coexistence region consists of mixtures of AFM and FM clusters, and it is metastable in nature. The lack of 'end point memory'' effect, as mentioned above, is a consequence of such metastability. On drawing a M–H curve in this metastable phase-coexistence region (obtained via FCC path) one introduces energy fluctuations, which drive the domains of metastable FM state to the stable AFM state. Such lack of 'end point memory' has been reported for the metastable regions across the magnetic transitions in $SmMn_2Ge_2$ (Roy *et al*., 2002). It should be mentioned here that the lack of 'end point memory' was also noticed earlier in the context of vortex solid–solid transition (Roy and Chaddah, 1997), but no

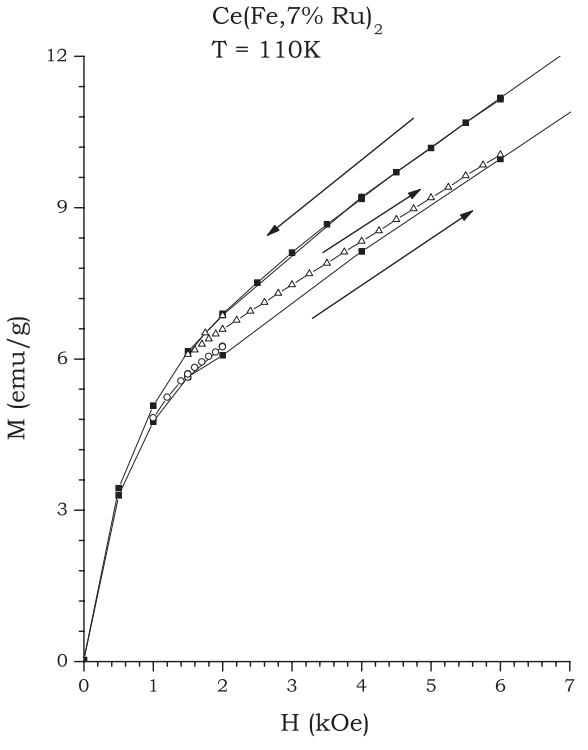

FIGURE 14 Comparison of minor hysteresis loops generated during ascending field cycle ($H = 2$ kOe – open circle) and descending field cycle ($H = 1.6$ kOe – open triangle) at approximately same value of magnetisation for Ce(Fe, 7% Ru)$_2$ at $T = 110$ K. The envelope curve is represented by solid squares (Manekar *et al.*, 2000b).

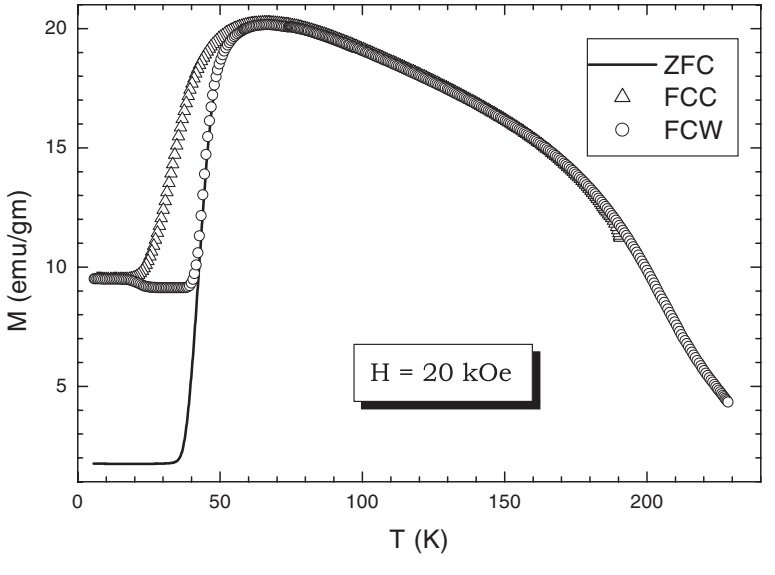

FIGURE 15 M vs. T plots for Ce($Fe_{0.96}Ru_{0.04}$)$_2$ alloy measured in ZFC, FCC and FCW protocols in an applied field of 20 kOe (Sokhey *et al.*, 2004).

Downloaded At: 12:30 28 January 2011

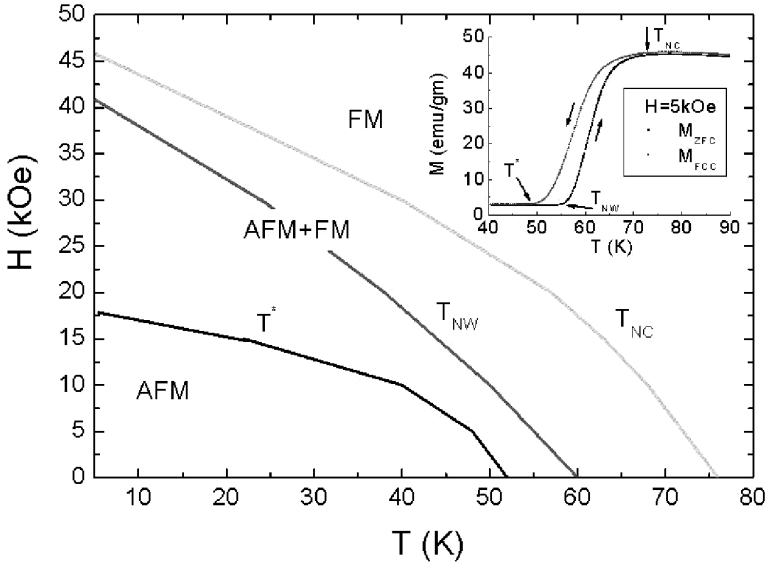

FIGURE 16 H–T phase diagram for $Ce(Fe_{0.96}Ru_{0.04})_2$ alloy representing T_{NW}, T_{NC} and T^* as a function of H. T_{NC} (T_{NW}) is marked as the point where M (T) shows a rapid rise (fall) while warming up (cooling down). T^* is the temperature where the $M_{ZFC}(T)$ and $M_{FCC}(T)$ curves meet at the low-temperature end (see inset). The value of T^* goes below 5 K (our lowest limit) when $H > 15$ kOe.

Downloaded At: 12:30 28 January 2011

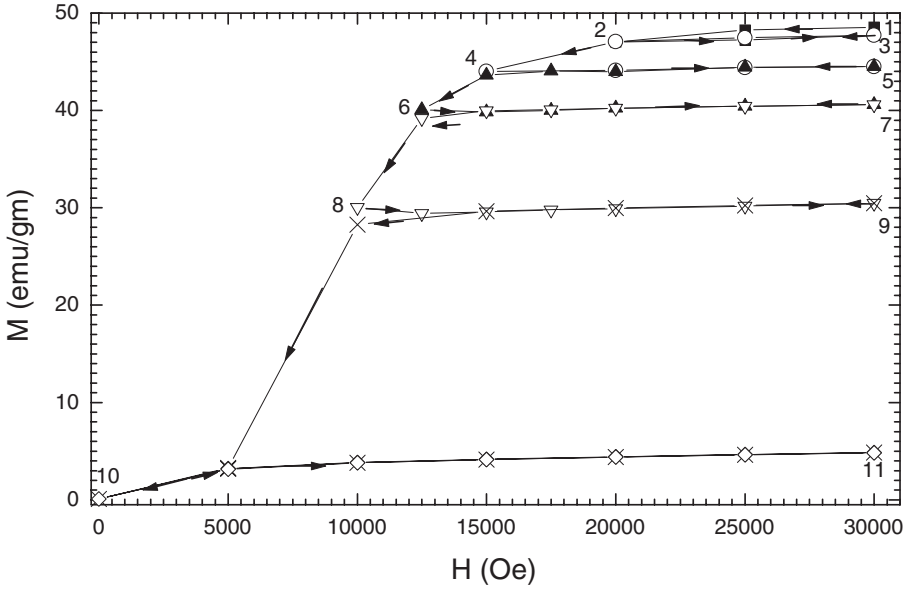

FIGURE 17 M–H curves drawn for $Ce(Fe_{0.96}Ru_{0.04})_2$ alloy at 5 K after field cooling in 30 kOe in the following successive cycles. $H = 30$ kOe $\rightarrow$ 20 kOe (path 1–2), 20 kOe $\rightarrow$ 30 kOe (path 2–3), 30 kOe $\rightarrow$ 15 kOe (path 3–4), 15 kOe $\rightarrow$ 30 kOe (path 4–5), 30 kOe $\rightarrow$ 12.5 kOe (path 5–6), 12.5 kOe $\rightarrow$ 30 kOe (path 6–7), 30 kOe $\rightarrow$ 10 kOe (path 7–8), 10 kOe $\rightarrow$ 30 kOe (path 8–9), 30 kOe $\rightarrow$ 0 kOe (path 9–10), 0 kOe $\rightarrow$ 30 kOe (path 10–11). Note the distinct lack of 'end point memory' at the end of each cycling path. Any further cycling after path 10–11 between 0 and 30 kOe traverses the same path reversibly (Sokhey *et al.*, 2004).

suitable explanation was put forward at that stage. Further support for the metastable nature of the phase-coexistence state has come from large relaxation of both in magnetisation and resistivity in the phase-coexistence regime (Chattopadhyay *et al.*, 2003; Sokhey *et al.*). Large relaxation behaviour is a characteristic feature of the phase-coexistence state in manganese oxides (Roy *et al.*, 2000a).

The question remains as to whether a superheated regime of the AFM state also exists in the H–T phase space of the present sample. Traditionally, superheating is relatively difficult to observe. However, some preliminary 'end point memory' tests indicate the presence of metastability in the H–T regime in Fig. 16 between T_{NW} and the $T^{**}(H)$ line (Sokhey *et al.*). In addition large magnetisation relaxation is observed in the same (H,T) region, which definitely indicates the presence of superheated AFM state (Chattopadhyay *et al.*, 2003).

5. ANOMALOUS ASPECTS OF FIRST-ORDER FM–AFM TRANSITION IN $CeFe_2$ ALLOYS: SIGNATURES OF KINETIC ARREST OF FOPT?

Downloaded At: 12:30 28 January 2011

The FM–AFM transition in doped $CeFe_2$ alloys is accompanied by a cubic to rhombohedral structural distortion (Kennedy and Coles, 1990). This magneto-structural coupling probably plays an important role in certain anomalous low-temperature properties of these alloys; these are particularly visible in Al-doped $CeFe_2$ alloys. In these alloys below 20 K the field-induced FM state does not revert back completely to the AFM state on withdrawal of the applied field (Manekar *et al.*, 2001). This gives rise to the striking feature of the ZFC virgin M–H curve lying out of the envelope M–H curve obtained by subsequent field cycling between $\pm H_{\max}$, where $H_{\max} \gg H_M$ (see Fig. 18). This anomalous feature is clearly reflected in the field dependence of resistivity as well (Singh *et al.*, 2002). The very similar behaviour has now been reported for CMR Mn-oxides (Dho and Hur, 2003) and magnetocaloric materials (Magen *et al.*, 2003). It is to be noted here that in these materials also the first-order FM–AFM magnetic transition is coupled with a structural change. As a possible explanation of the observed anomalous features we introduce the idea that the kinetics of the FM to AFM transition is arrested at a low T and high H (Manekar *et al.*, 2001). We recognise that for (H,T) values below the (H^*,T^*) band the free energy barrier separating the FM from the AFM phase has dropped to zero throughout the sample. An infinitesimal fluctuation should drive any FM region to the AFM phase. But all our observations indicate that at a very low T the (unstable) FM regions remain in the AFM phase. It is well known that at a sufficiently low T the characteristic time for structural relaxation becomes longer than experimental time scales (Debenedetti, 1996). We postulate that at a sufficiently low T the displacive motion of atoms involved in the structural distortion that is associated with the FM–AFM transition in the 4% Al-doped $CeFe_2$ sample becomes negligible on experimental time scales. The high-temperature high-field FM phase is then frozen in. We accordingly postulate that below a certain temperature $T_K(H)$ the kinetics of the FM–AFM transformation is hindered and arrested just like in a quenched metglass. This is similar to observations at high pressures where the high-density phase cannot transform (Sharma and Sikka, 1996) to the low-density phase below a certain T_K, with T_K rising as the pressure rises. The metastable state thus obtained will have qualitatively different features from the usual phase-coexistence regime expected across the disorder-influenced first-order transition. Preliminary

studies on magnetocaloric material Gd_5Ge_4 have brought out this difference in 'end point memory effect' and in magnetic relaxation studies (Chattopadhyay *et al.*), and further studies are in progress.

6. CONCLUSION

The actual composition in any alloy or doped compound varies around some average composition simply due to the disorder that is frozen in as the solid crystallises from the melt. It was proposed earlier (Imry and Wortis, 1979) that such static, quenched in, purely statistical compositional disorder can under certain circumstances introduce a landscape of transition temperature in a system undergoing first-order transition.

Downloaded At: 12:30 28 January 2011

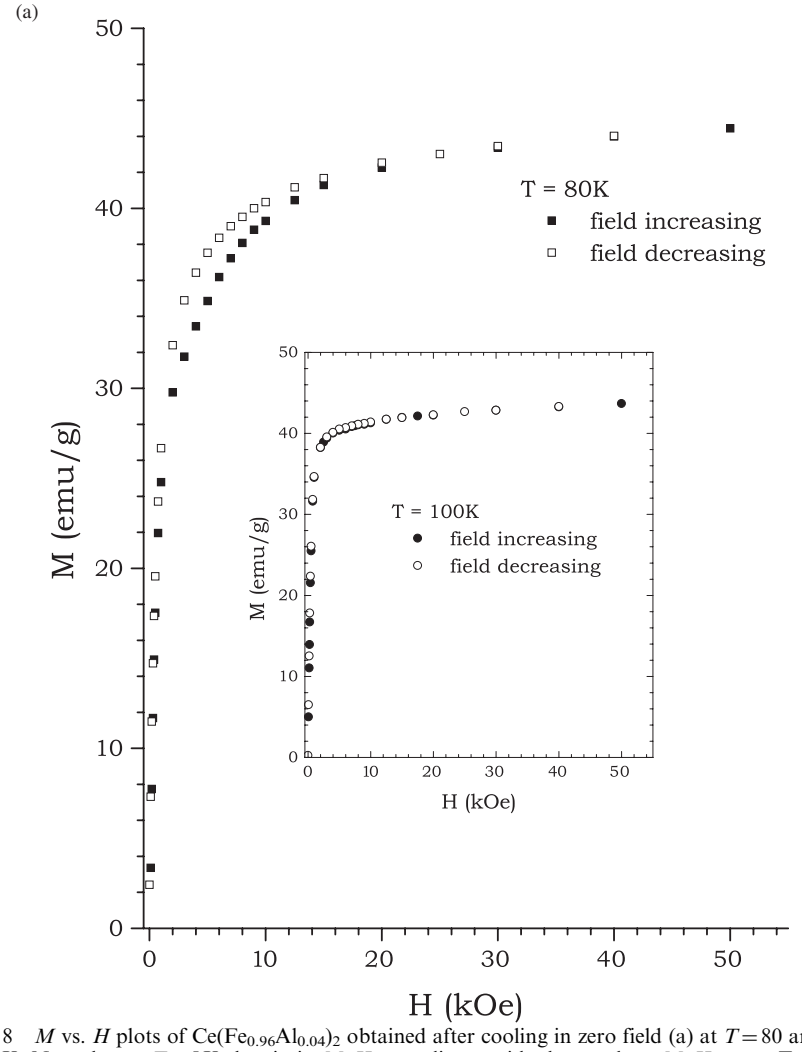

FIGURE 18 M vs. H plots of $Ce(Fe_{0.96}Al_{0.04})_2$ obtained after cooling in zero field (a) at $T=80$ and 100 K (b) at $T=5$ K. Note that at $T=5$ K the virgin M–H curve lies outside the envelope M–H curve. To confirm this anomalous nature of a virgin curve we have also drawn this in the negative field direction after zero-field cooling the sample (Manekar *et al.*, 2001).

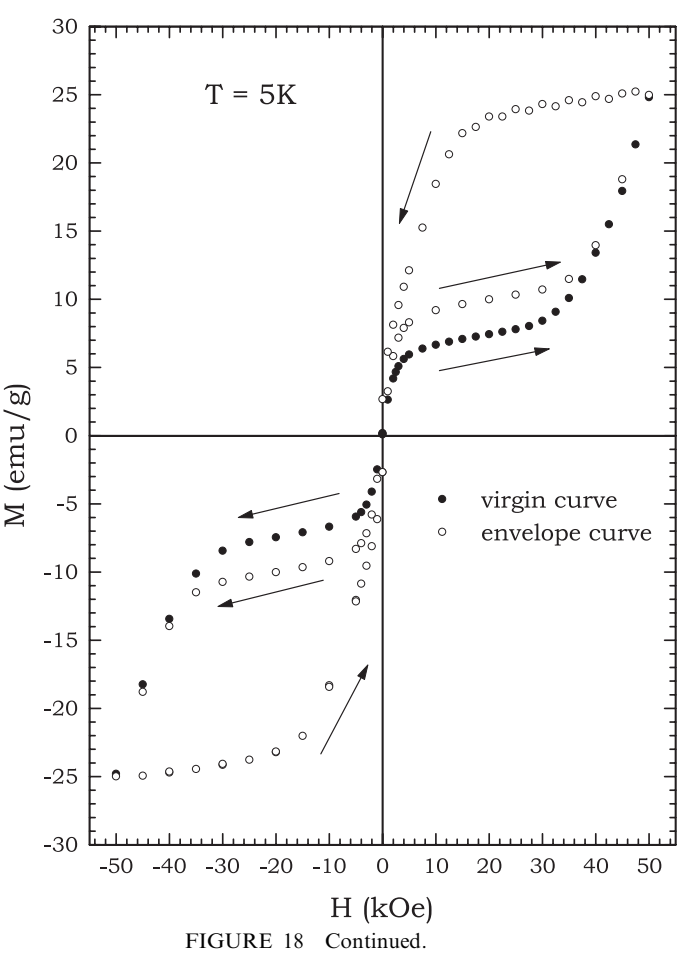

FIGURE 18 Continued.

Downloaded At: 12:30 28 January 2011

Detailed computational studies (Moreo *et al.*, 2000; Dagotto *et al.*, 2001) confirm the applicability of such a picture in CMR Mn-oxide compounds and further emphasise that phase coexistence can occur in any system in the presence of quenched disorder whenever two states are in competition through a first-order phase transition. Through our experimental studies on vortex matter and a test-bed magnetic system, namely $CeFe_2$ alloys, and comparing the results with other vortex matter systems and magnetic materials, we support this picture and highlight the fact that phase coexistence and metastability are universal characteristics of a disorder-influenced FOPT. We have also highlighted certain features, which points towards the kinetics of the FOPT process, which remains to be understood properly. In this respect a relatively simple magnetic system like $CeFe_2$ provides an excellent context for the study of first-order transition processes in general: experimentally, it is far easier to explore H–T phase space than it is to use pressure as a variable. With the appropriate experimental probe and samples with controlled disorder, it will be possible to study the generalised phenomena of nucleation (heterogeneous versus homogeneous) and growth kinetics in first-order transition processes, and also their possible path dependence in the phase space defined in terms of the control variables.

Acknowledgements

We thank M.A. Manekar and Dr. M.K. Chattopadhyay for critical reading of the manuscript and useful discussions.

References

Angst, M. *et al.* (2003). Disorder-induced phase transition of vortex matter in MgB_2. *Phys. Rev.*, **B67**, 12502.
Avraham, N. *et al.* (2001). Inverse melting of vortex lattice. *Nature*, **411**, 451.
Bean, C.P. and Rodbell, D.S. (1962). Magnetic disorder as a first-order phase transformation. *Phys. Rev.*, **126**, 104.
Blatter, G. (1997). *Vortex matter Physica*, **C282–287**, 19.
Blatter, G. *et al.* (1994). Vortices in high-temperature superconductors. *Rev. Mod. Phys.*, **66**, 1125.
Burgy, J. *et al.* (2001). Colossal effects in transition metal oxides caused by intrinsic inhomogeneities. *Phys. Rev. Lett.*, **87**, 277202.
Chaddah, P. *et al.* (1992). Minor hysteresis loops and harmonic generation calculations in a generalized critical-state model. *Phys. Rev.*, **B46**, 11737.
Chaddah, P. and Roy, S.B. (1999). Supercooling across first-order phase transitions induced by density variation. *Phys. Rev.*, **B60**, 11926.
Chaddah, P. and Roy, S.B. (2000). Supercooling across first-order phase transitions in vortex matter. *Pramana*, **54**, 857.
Chaikin, P.M. and Lubensky, T.C. (1995). *Principles of Condensed Matter Physics*. Cambridge University Press, Cambridge.
Chattopadhyay, M.K. *et al.* (2003). Metastability and giant relaxation across the ferromagnetic to antiferromagnetic transition in $Ce(Fe_{0.96}Ru_{0.04})_2$. *Phys. Rev.*, **B68**, 174404.
Chattopadhyay, M.K. *et al.* (unpublished).
Chattopadhyay, M.K., Manekar, M.A. Roy, S.B. and Chaddah, P. (to be published).
Chaudhary, S. *et al.* (2000a). History dependence of peak effect in $CeRu_2$ and V_3Si: an analogy with the random field Ising systems. *Solid St. Commun.*, **114**, 5.
Chaudhary, S. *et al.* (2000b). Peak effect in the superconducting mixed state of bulk Mo-Re alloys: a dc magnetization study. *Philos. Mag.*, **B80**, 1393 (and references there in).
Dagotto, E., Hotta, T. and Moreo, A. (2001). *Phys. Rep.* **344**, 1; Dagatto, E. (2003). *The Physics of Manganites and Related Compounds*. Springer (and references there in).
Debenedetti, P.G. (1996). *Metastable Liquids*, Chapter 4. Princeton University Press, Princeton, New Jersey.
Dho, J. and Hur, N.H. (2003). Thermal relaxation of field-induced irreversible ferromagnetic phase in Pr-doped manganites. *Phys. Rev.*, **B67**, 214414.
Freitas, R.S. *et al.* (2002). Magnetization studies of phase separation in $La_{0.5}Ca_{0.5}MnO_3$. *Phys. Rev.*, **B65**, 104403.
Giller, D. *et al.* (2000). Transient vortex states in $Bi_2Sr_2CaCu_2O_{8+\ delta}$ crystal. *Phys. Rev. Lett.*, **84**, 3698; van der BecK, C.J. *et al.* (2000). Supercooling of the disordered vortex lattice in $Bi_2Sr_2CaCu_2O_{8+delta}$. *Phys. Rev. Lett.*, **84**, 4196; Gaifullian, M.B. *et al.* (2000). Abrupt change of Josephson plasma frequency at the phase boundary of the bragg glass in $Bi_2Sr_2CaCu_2O_{8+\ delta}$. *Phys. Rev. Lett.*, **84**, 2945.
Imry, Y. and Wortis, M. (1979). Influence of quenched impurities on first-order phase transition. *Phys. Rev.*, **B19**, 3580.
Kennedy, S.J. and Coles, B.R. (1990). The magnetic phases of pseudobinary $Ce(Fe_{1-x}M_x)_2$ intermetallic compounds; M=Al, Co, Ru. *J. Phys.: Condens. Matter*, **2**, 1213.
Kimura, T. *et al.* (1999). Diffuse phase transition and phase separation in Cr-Doped $Nd_{1/2}Ca_{1/2}MnO_3$: a relaxor ferromagnet. *Phys. Rev. Lett.*, **83**, 3940; Parisi, F. *et al.* (2001). Magnetoresistance induced by low-field control of phase separation in $La_{0.5}Ca_{0.5}MnO_3$. *Phys. Rev.*, **B63**, 144419.
Kunkel, H. *et al.* (1996). Giant magnetoresistive behavior near the metamagnetic transition in $Ce(Fe_{0.93}Ru_{0.07})_2$. *Phys. Rev.*, **B53**, 15099; Fukuda, H. *et al.* (2001). Magnetic and transport properties of the pseudobinary systems $Ce(Fe_{1-x}Co_x)_2$ and $(Ce_{1-y}Sc_y)Fe_2$. *Phys. Rev.*, **B63**, 054405.
Kupfer, H. *et al.* (2003). Correlation of the vortex order-disorder transition with the symmetry of the crystal lattice in V_3Si. *Phys. Rev.*, **B67**, 6407.
Kwok, W.K. *et al.* (1994). Vortex liquid disorder and the first order melting transition in $YBa_2Cu_3O_{7\text{-}delta}$. *Phys. Rev. Lett.*, **72**, 1092.
Ling, X.S. *et al.* (2001). Superheating and supercooling of vortex matter in a Nb single crystal: direct evidence for a phase transition at the peak effect from neutron diffraction. *Phys. Rev. Lett.*, **86**, 712; Park, S.R. *et al.* (2003). Fate of the peak effect in a Type-II superconductor: multicriticality in the Bragg-glass transition. *Phys. Rev. Lett.*, **91**, 167003.
Magen, C. *et al.* (2003). Magnetoelastic behaviour of Gd_5Ge_4. *J. Phys.:Condens. Matter.*, **15**, 2389.

Downloaded At: 12:30 28 January 2011

Manekar, M.A. *et al.* (2001). First-order transition from antiferromagnetism to ferromagnetism in $Ce(Fe_{0.96}Al_{0.04})_2$. *Phys. Rev.*, **B64**, 104416.
Manekar, M.A., Roy, S.B. and Chaddah, P. (2000a). First-order transition from ferromagnetism to antiferromagnetism in $CeFe_2$-based pseudobinary alloys. *J. Phys. Condens. Matter* **12**, L409.
Manekar, M.A. *et al.* (2000b). First-order metamagnetic transition in $CeFe_2$-based pseudobinary alloys. *J. Phys. Condens. Matter.*, **12**, 9645.
Moreo, A. *et al.* (2000). Giant cluster coexistence in doped manganites and other compounds. *Phys. Rev. Lett.*, **84**, 5568.
Paltiel, Y. *et al.* (2000). Instabilities and disorder-driven first-order transition of the vortex lattice. *Phys. Rev. Lett.*, **85**, 3712; Paltiel, Y. *et al.* (2000). Dynamic instabilities and memory effects in vortex matter. *Nature*, **403**, 398.
Paolisini, L. *et al.* (1998). Magnetic response function of the itinerant ferromagnet $CeFe_2$. *Phys. Rev.*, **B58**, 12117 (and references therein).
Pecharsky, V. *et al.* (2003). Massive magnetic-field-induced structural transformation in Gd_5Ge_4 and the nature of the giant magnetocaloric effect. *Phys. Rev. Lett.*, **91**, 197204.
Pippard, A.B. (1969). *Philos. Mag.*, **19**, 217.
Radzyner, Y. *et al.* (2000). Metastable vortex states in $YBa_2Cu_3O_{7-\ delta}$ crystal. *Phys. Rev.*, **B61**, 14362.
Radzyner, Y., Shaulov, A. and Yeshurun, Y. (2002). Unified order-disorder vortex phase transition in high-T_c superconductors. *Phys. Rev.*, **B65**, 100513.
Ravikumar, G. *et al.* (1999). Step change in equilibrium magnetization across the peak effect in 2H-$NbSe_2$. *Physica*, **C322**, 145.
Ravikumar, G. *et al.* (2000). Supercooling of the disordered vortex phase via minor hysteresis loops in 2H-$NbSe_2$. *Phys. Rev.*, **B61**, 12490.
Roy, S.B. *et al.* (1999). Nonequilibrium behaviour in the field-cooled magnetization of the C15 laves-phase superconductor $CeRu_2$. *Solid St. Commun.*, **109**, 427.
Roy, S.B. *et al.* (2002). Interesting thermomagnetic history effects in the antiferromagnetic state of $SmMn_2Ge_2$. *J. Phys.: Condens. Matter.*, **14**, 9779.
Roy, S.B. and Chaddah, P. (1997). Study of minor hysteresis loops in the usual and anomalous superconducting regime of $(Ce_{0.95}Nd_{0.05})Ru_2$: evidence of a first-order transition. *Physica*, **C279**, 70.
Roy, S.B. and Chaddah, P. (1997). Anomalous superconducting response in $CeRu_2$ and $(Ce_{0.95}Nd_{0.05})Ru_2$: evidence of a first-order transition. *J. Phys.: Condens. Matter*, **9**, L625.
Roy, S.B. and Chaddah, P. (1999). Sample dependence of the normal state magnetic properties in $CeRu_2$ and possible correlations with the anomalous superconducting response. *Physica*, **B262**, 20.
Roy, S.B. and Coles, B.R. (1989). On the instability of ferromagnetism in $CeFe_2$: effects of alloying with Al, Mn, Y and U. *J. Phys.: Condens. Matter*, **1**, 419.
Roy, S.B. and Coles, B.R. (1990). Magnetic behavior of $CeFe_2$: Effects of Ru, Rh, and Pd substitutions. *Phys. Rev.*, **B39**, 9360.
Roy, S.B., Chaddah, P. and DeLong, L.E. (1998a). Possibility of a first-order transition in the magnetization study of the anomalous superconducting mixed state of $CeRu_2$. *Physica*, **C304**, 43.
Roy, S.B., Chaddah, P. and Chaudhary, S. (1998b). The anomalous mixed state of the C15-laves phase superconductor $CeRu_2$: II. History dependence in field-cooled magnetization hysteresis. *J. Phys.: Condens Matter*, **20**, 8327.
Roy, M., Mitchell, J.F. and Schiffer, P. (2000a). Time dependent effects and transport evidence for phase separation in $La_{0.5}Ca_{0.5}MnO_3$. *J. Appl. Phys.*, **87** 5831.
Roy, S.B., Chaddah, P. and Chaudhary, S. (2000b). Peak effect in $CeRu_2$: history dependence and supercooling. *Phys. Rev.*, **B62**, 9191.
Roy, S.B., Chaudhary, S., Chaddah, P. and Cohen, L.F. (1999). Anomalous magnetization in the superconducting mixed state of $CeRu_2$: a study with vibrating sample magnetometer. *Physica*, **C322**, 115.
Safar, H. *et al.* (1992) Experimental evidence for a first-order vortex-lattice-melting transition in untwinned, single crystal $YBa_2Cu_3O_7$. *Phys. Rev. Lett.*, **69**, 824.
Sharma, S.M. and Sikka, S.K. (1996). *Prog. Mater. Sci.*, **40**, 1.
Singh, K.J. *et al.* (2002). First-order transition from ferromagnetism to antiferromagnetism in $Ce(Fe_{0.96}Al_{0.04})_2$: a magnetotransport study. *Phys. Rev.*, **B65**, 94419.
Soibel, A. *et al.* (2000). Imaging the vortex-lattice melting process in the presence of disorder. *Nature* (*London*), **406**, 283.
Sokhey, K.J.S. *et al.* (2004). Signatures of phase separation across the disorder broadened first order ferromagnetic to antiferromagnetic transition in doped-$CeFe_2$ alloys. *Solid St. Commun.*, **129**, 19.
Sokhey, K.J.S., Chattopadhyay, M.K., Manekar, M.A., Roy, S.B. and Chaddah, P. (to be published).
Vinokur, V.M. *et al.* (1998). Lindemann criterion and vortex-matter phase transitions in high-temperature superconductors. *Physica*, **C295**, 209.
White, R.M. and Geballe, T.H. (1979). *Long Range Order in Solids.* Academic Press, New York.
Zhukov, A.A. *et al.* (2001). History effects and phase diagram near the lower critical point in $YBa_2Cu_3O_7$ single crystals. *Phys. Rev. Lett.*, **87**, 017006.

Downloaded At: 12:30 28 January 2011